Marine Geology 279 (2011) 199–209

Contents lists available at ScienceDirect

Marine Geology

journal homepage: www.elsevier.com/locate/margeo

Estimation of high-resolution sediment concentration profiles in bottom boundary layer using pulse-coherent acoustic Doppler current profilers

H.K. Ha [a,*], J.P.-Y. Maa [b], K. Park [c], Y.H. Kim [d,1]

[a] Korea Polar Research Institute, Songdo Technopark, Incheon 406-840, South Korea
[b] Department of Physical Sciences, Virginia Institute of Marine Science, School of Marine Science, College of William and Mary, Gloucester Point, VA 23062, USA
[c] Department of Marine Sciences, University of South Alabama, Dauphin Island Sea Lab., Dauphin Island, AL 36528, USA
[d] Horn Point Laboratory, University of Maryland Center for Environmental Science, Cambridge, MD 21613, USA

ARTICLE INFO

Article history:
Received 27 April 2010
Received in revised form 4 November 2010
Accepted 4 November 2010
Available online 12 November 2010

Communicated by D.J.W. Piper

Keywords:
ADCP
pulse-coherent mode
backscatter
suspended sediment concentration
bottom boundary layer

ABSTRACT

The capability of two acoustic profilers — SonTek's 1.5-MHz pulse-coherent acoustic Doppler profiler (PC-ADP) and RDI's 600-kHz acoustic Doppler current profiler (ADCP) with pulse-coherent mode — was evaluated for estimating high-resolution suspended sediment concentration (SSC) profiles in bottom boundary layer. In the laboratory measurements with a PC-ADP, two types of sediments were tested to study acoustic responses to grain size. A natural sediment sample from Clay Bank, a mixture of clay and very fine sand, showed a good linear relationship between range-corrected volume scattering ($\overline{S_v}$) and backscattered strength (E) until SSC increased up to about 10 g l^{-1}. In contrast, a commercially available kaolinite exhibited earlier signal saturation and non-unified linear regressions between $\overline{S_v}$ and E, most likely because the particle size is much smaller than the transmitted acoustic wavelength. Using a pulse-coherent ADCP, the field measurement results from Mobile Bay, Alabama showed that the acoustically-derived SSC profiles were well matched with the optically-derived outcomes although slight discrepancies were noted. The overestimation of acoustically-derived SSC near the bed may be related to the side lobe interference near the bed and the enhanced acoustic sensitivity by coarser particles and denser aggregates eroded from the bed. Mean absolute error of acoustic estimates was within 4.1–7.3% of the optically-derived SSC range, which is attributable to the different acoustic and optical scattering responses to given sediment size spectra. Despite some error sources in acoustic inversion, the results from laboratory and field experiments suggest that the pulse-coherent acoustic profiler is able to reveal the evolution of in-situ near-bed SSC profiles with high vertical and temporal resolutions.

1. Introduction

Accurate measurement of suspended sediment concentration (SSC) profiles is an important task to understand sediment dynamics in estuarine and coastal environments. During the last few decades, considerable efforts have been dedicated to develop SSC-measuring techniques and to increase the data accuracy (see Wren et al., 2000 for review). Although the optical instruments, e.g., optical backscatter sensor (OBS), have been developed and widely used to estimate the SSC (Downing, 2006; Downing and Beach, 1989; Ha and Maa, 2009; Kineke and Sternberg, 1992; Sternberg et al., 1986, Sutherland et al., 2000), their measurements are restricted to a fixed coordinate that can only be claimed as a single point. In order to increase the spatial resolution of SSC measurements, multiple optical sensors need to be deployed at the target depths. Multiple probes, however, may disturb the structure of turbulent flow as well as the distribution of suspended solids, especially when deployed in the vicinity of the sediment bed. These drawbacks consistently shed new light on the acoustic measuring system as an alternative for estimating SSC profiles in bottom boundary layer (BBL) where both velocity and SSC exhibit the largest vertical gradients (Friedrichs et al., 2000; Thorne and Hanes, 2002).

As a non-intrusive method, the acoustic instruments have been used for obtaining SSC profiles in both laboratories (Admiraal and Garcia, 2000; Betteridge et al., 2008; Thorne et al., 1991) and field sites (Gartner, 2004; Hamilton et al., 1998; Hanes et al., 1988; Mouraenko, 2004; Shi et al., 1999). An acoustic backscatter sensor (ABS; Aquatec, 2006) with multi-frequency transducers has become commercially available for measuring the profiles of SSC and particle size. Most sediment dynamics studies, however, require the knowledge of applied flow conditions to reveal the sediment transport and fate, so that a current meter needs to be deployed simultaneously with an ABS. In order to meet such demands on the concurrent measurement of velocity and SSC profiles, an acoustic Doppler current profiler (ADCP) with incoherent single pulse has been attempted (Gartner, 2004; Hill et al., 2003; Holdaway et al., 1999; Kim and Voulgaris, 2003; Land and Jones, 2001; Land et al., 1997). While the primary function of an ADCP is to provide time series of velocity profiles, the strength of acoustic backscattered signals can be used as a proxy to estimate SSC profiles. Even though the single-pulse

* Corresponding author. Tel.: +82 32 260 6185; fax: +82 32 260 6109.
E-mail addresses: ha@kopri.re.kr, hokyung.ha@gmail.com (H.K. Ha).
[1] Present address: Applied Science Associates, Inc., South Kingstown, RI 02879, USA.

0025-3227/$ – see front matter © 2010 Elsevier B.V. All rights reserved.
doi:10.1016/j.margeo.2010.11.002

systems have successfully measured the changes in velocity and SSC within a relatively long (10–100 m) profiling range, the spatial resolution is too coarse to resolve BBL dynamics due to the inherent limitation on attainable cell (or bin) size.

Pulse-coherent acoustic profilers have recently emerged for collecting high-resolution, high-frequency velocity profiles in BBL (RDI, 2003; Smyth et al., 2002; SonTek, 2001a; Zedel et al., 1996). They are designed to transmit a pair of pulses with a certain time lag, and utilize the phase change between the two pulses to measure the flow velocity (RDI, 2003; SonTek, 2001a,b). The salient advantage of the pulse-coherent mode over the incoherent mode is to provide a profiling capability with fine vertical resolution (down to 0.01–0.02 m) and low noise level, so that the pulse-coherent ADCP would not suffer from the constraint on cell size and short-term accuracy inherent to the pulse-incoherent ADCP (Lohrmann et al., 1990). In this respect, the pulse-coherent acoustic profiler has a merit to non-intrusively monitor sediment dynamics in BBL with fine resolutions. Despite these prospective features, most previous works have focused on the pulse-coherent operational theories (Lhermitte and Serafin, 1984; Zedel et al., 1996) and the application to hydrodynamic measurements (Lacy and Sherwood, 2004; Lohrmann et al., 1990; Lorke and Wuest, 2005). Little is known about the capability and accuracy of pulse-coherent ADCPs for estimating the SSC profiles in BBL.

This study evaluated the capability of two pulse-coherent acoustic profilers in estimating near-bed SSC profiles in comparison to the outcomes derived from optical sensors as well as water samples. A theoretical overview for acoustic backscattering is given in Section 2, followed by the description of the experimental settings in Section 3. Calibration and two profiling tests in a laboratory water tank and an in-site moored site are described in Section 4. In Section 5, the effect of different size spectra of each sediment group on the acoustic responses is discussed, and the uncertainties and error sources in acoustic measurement and signal processing are discussed.

2. Acoustic backscattering theory

Since the acoustic technique is an indirect method, the measured backscattered signals should be calibrated to convert to SSC. The important task in calibration is to consider the range- and SSC-dependent sound attenuation. Below is a brief overview of the determination of sound attenuation coefficient and the basics of acoustic inversion algorithm for estimating SSC profiles.

2.1. Sound attenuation coefficient

Sound is exponentially attenuated with distance from a source transducer (Urick, 1983). The attenuation coefficient is a function of various parameters including temperature, pressure, salinity, frequency and the suspended sediment properties, e.g., size, shape, mineralogy and SSC (Richards et al., 1996). The total sound attenuation coefficient (α) is bipartite: the attenuation by water (α_w) and by suspended sediments (α_s). The coefficient α_w was empirically formulated by several authors (e.g., Fisher and Simmons, 1977), and the subroutine for calculating α_w is easily found in acoustic communities (e.g., Kinsler et al., 2000). As the acoustic frequency increases, α_w would generally increase and the difference in the attenuation coefficient between salty water and freshwater decreases (Medwin and Clay, 1998). The attenuation by sediments, α_s, becomes important in the near-bed, high-concentration layer, and is determined by the SSC in the sensing range (R), the sub-distance from an emitter (r) and two sound absorption components of the scattering loss (ξ_s) and the viscous absorption (ξ_v) (Richards et al., 1996):

$$\alpha_s = \frac{1}{R}\int_0^R (\xi_s + \xi_v) SSC(r) dr. \tag{1}$$

More details on these two absorption components, which are functions of frequency and grain size, can be found in Thorne et al. (1991) and Thorne and Hanes (2002). The variations in total attenuation, $\xi = (\xi_s + \xi_v)$, are shown in Fig. 1. At the frequency of 1.5 MHz, for example, ξ_s is dominant for large particles with mean grain size (d_{50}) > 100 μm, whereas ξ_v becomes important for fine-grained particles with d_{50} < 100 μm (Fig. 1b). The total sediment attenuation

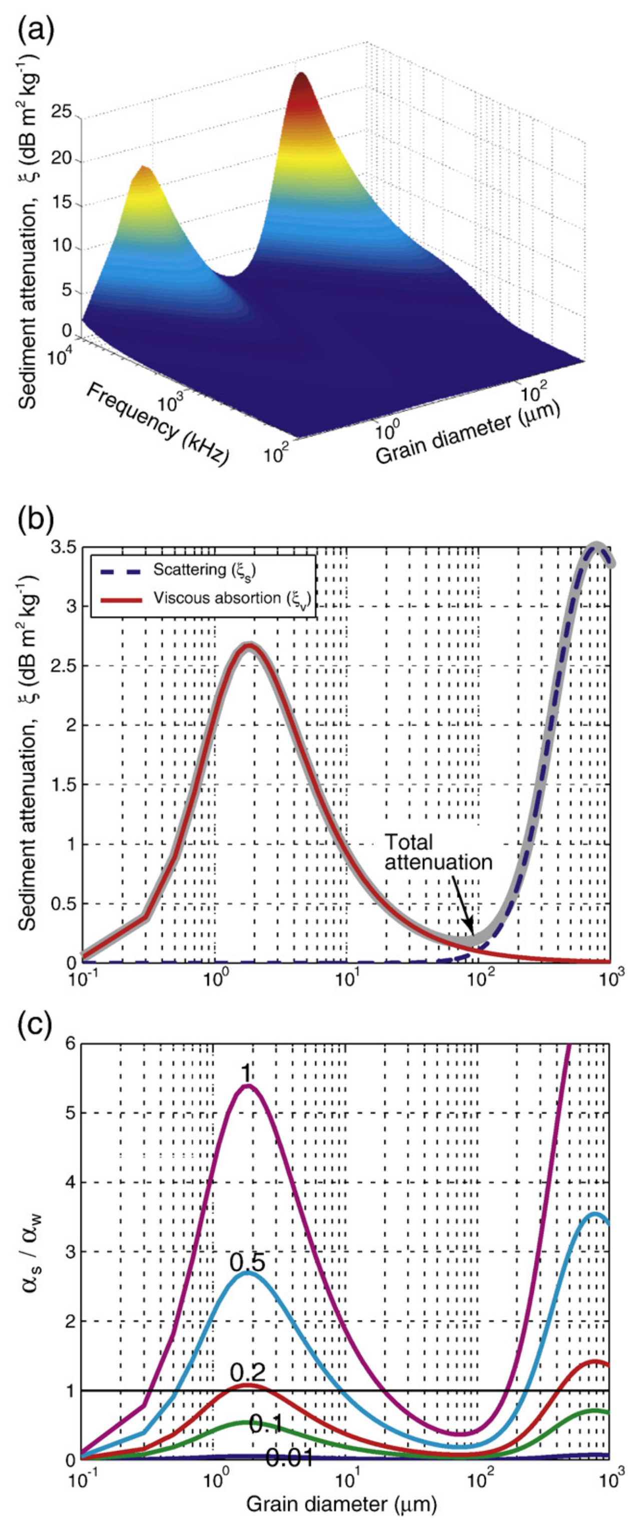

Fig. 1. (a) Total sound attenuation (ξ) by scattering loss (ξ_s) and viscous absorption (ξ_v); (b) ξ_s and ξ_v at 1.5 MHz; and (c) the ratio of sound attenuation by sediment (α_s) to that by water (α_w) at 1.5 MHz. The numbers in (c) indicate the SSC in g l^{-1}.

exhibits peaks at $d_{50} \approx 2$ and 800 μm. Since the second peak is caused by scattering wave for large particles around 800 μm, it is out of the interested range for fine, cohesive sediments, and thus, not addressed in this study. For low SSC (<ca. 0.01 g l^{-1}), α_s is negligibly small compared with α_w (Fig. 1c). For $d_{50} \approx 2$ μm, α_s becomes larger than α_w when SSC is higher than about 0.2 g l^{-1}. When the SSC is 0.5 g l^{-1}, α_s is about 2.8 times greater than α_w. This indicates that, unlike the application to the water column with low SSC, α_s must be taken into account when estimating the SSC in BBL where SSC is relatively high due to the frequent erosion and resuspension of bed sediments.

2.2. Acoustic inversion algorithm

The backscattered signal strength is mainly dependent on (1) setup options of selected acoustic system and (2) properties of suspended sediment (Urick, 1983). The first includes the acoustic wave frequency, transmit power, sensor sensitivity and other system settings. They are usually known, set by manufacturers or fixed by users. The second, on the other hand, is associated with the concentration, size and type of suspended sediment particles. Physical parameters of water such as temperature and salinity also have secondary effects. Because the acoustic responses exhibit a site (or sediment)-specific feature, the backscattered signal strength must be calibrated against sample concentration from a deployed site to obtain the SSC or its profile (Kawanisi and Yokosi, 1997; Thorne and Hanes, 2002).

For extending the application of ADCPs to estimate SSC profiles, the sonar equation was simplified by Deines (1999), and subsequently modified to include α_s for high SSC profiles (Ha, 2008; Kim et al., 2004).

$$S_v = K_c(E-E_r) + 2(\alpha_w + \alpha_s)R + 10\cdot\log(R^2) - 10\cdot\log(PL) - 10\cdot\log(P) + C \quad (2)$$

where $S_v = 10\cdot\log(SSC/SSC_r)$ is the volume scattering strength (dB) expressing the density of scattering within a volume, SSC_r is the reference concentration, K_c is a signal calibration coefficient, E is the echo level (count), E_r is the noise level, PL is the transmit pulse length, P is the transmit power and C is another calibration coefficient (see Eqs. 2 and 6 in Deines (1999)). Because SSC_r, E_r, PL, P and C can be fixed during a calibration experiment, Eq. (2) can be further simplified by introducing a new calibration coefficient C' that incorporates all the fixed parameters:

$$\overline{S_v} = K_c E + C' \quad (3)$$

where $\overline{S_v} = 10\cdot\log(SSC) - 2(\alpha_w + \alpha_s)R - 10\cdot\log(R^2)$, the net volume scattering corrected by subtracting the sound spreading and attenuation in the sensing range.

If true SSCs at several levels in the sensing range are simultaneously measured by other means, the two calibration coefficients can be determined by linear regression: K_c from the slope and C' from the y-intercept (Deines, 1999; Kim et al., 2004; Traykovski et al., 2007). When in-situ samples are not available, a laboratory mixing chamber that can generate a homogeneous suspension is another common approach (Mouraenko, 2004; Thorne and Hanes, 2002; Thorne et al., 1991). It should be noted that it is impossible to directly estimate the entire SSC profile using Eq. (2) because α_s is also a function of SSC. Through the iterative calculation with known calibration coefficients, however, SSC and α_s at each cell can be sequentially computed (Lee and Hanes, 1995; Thorne and Hanes, 2002). More details on signal inversion can be found in Thorne and Hanes (2002) and Ha (2008).

3. Materials and methods

3.1. Pulse-coherent acoustic Doppler current profiler (PC-ADCP)

The pulse-coherent technology was originally developed for acoustic Doppler velocimeters (ADVs), a single-point velocity measurement device, and was later transplanted in ADCPs to produce high-precision velocity profiles with small cells and rapid sampling rates (SonTek, 2001b). Pulse-coherent acoustic profilers transmit two consecutive pulses to measure the flow velocity profiles. The phase change between the two pulses is utilized in the signal processing for calculating velocity profiles, whereas a single-pulse ADCP utilizes the frequency shift, i.e., Doppler shift, between transmitted acoustic wave and backscattered return wave (RDI, 2003; SonTek, 2001a,b). The time lag between two consecutive pulses determines the maximum resolvable velocity and profiling range (RDI, 2002; SonTek, 2001b). A tradeoff exists between such parameters: as the time lag increases, the profiling range increases, but the maximum detectable velocity decreases. Pulse-coherent systems would operate with a much shorter pulse length (ca. 0.01–0.02 m), which could reduce the signal-to-noise ratio by about 15 dB (SonTek, 2001b). The operational mechanisms mentioned above make it possible to obtain high-resolution, high-frequency profiles of current velocity and SSC derived from the backscattered strength over a short range (1–2 m). Pulse-coherent systems, therefore, are suitable for investigating sediment dynamics in BBL (Lacy and Sherwood, 2004).

There are several acoustic current profilers with pulse-coherent technology in the commercial market. Although the operational theory is the same, an individual company has its own brand name due to the trademark and patent. We tested two instruments in this study, SonTek's 1.5-MHz PC-ADP and RDI's 600-kHz WorkHorse ADCP with mode 11 (i.e., pulse-coherent mode; RDI, 2003). These two profilers will be hereafter referred to as "PC-ADCP," as a unified name, unless otherwise specified. SonTek's PC-ADP, having three transducers equally spaced at 120° relative azimuth angles, was tested in a laboratory calibration chamber and a settling tank. RDI's ADCP, having four transducers placed in the Janus beam geometry, was tested in Mobile Bay, Alabama. Table 1 summarizes the configuration and selected setups of the two PC-ADCPs.

3.2. Sediments

In the laboratory measurements, two types of sediments were used: a natural sediment sample from Clay Bank area, the York River, Virginia and a commercially available kaolinite. The Clay Bank sediment showed a bimodal distribution (Fig. 2a). The first mode (ca. 0.7 μm) and the second mode (ca. 88 μm) were found in clay and very fine sand range, respectively (Table 2). In contrast, the kaolinite showed a unimodal distribution with $d_{50} \approx 0.7$ μm (Fig. 2b). The suspended sediments in Mobile Bay mainly consisted of clay and silt (Table 2 and Fig. 2c). The distribution was unimodal with $d_{50} \approx 9.8$ μm.

Table 1
Configuration and selected setups of the two pulse-coherent acoustic current profilers used in this study.

	SonTek's PC-ADP	RDI's ADCP
Configuration		
Frequency (kHz)	1500	600
Transducer type	Monostatic	Monostatic
Transducer diameter (m)	0.02	0.1
Transducer number	3	4
Beamwidth at −3 dB (°)	1.85	1.5
Slant angle (°)	15	20
Minimum cell size (m)	0.016	0.02
Wavelength[a] (mm)	1	2.5
Selected setups		
Cell size (m)	0.047	0.1
Blanking distance (m)	0.15	0.5
Profiling rate (Hz)	2	2
Selected ping mode	Pulse-coherent mode	Mode 11[b]
Tested area	Laboratory tank	Mobile Bay, AL

[a] Assuming that sound speed in water is 1500 m s^{-1}.
[b] Mode 11 is equivalent to pulse-coherent mode.

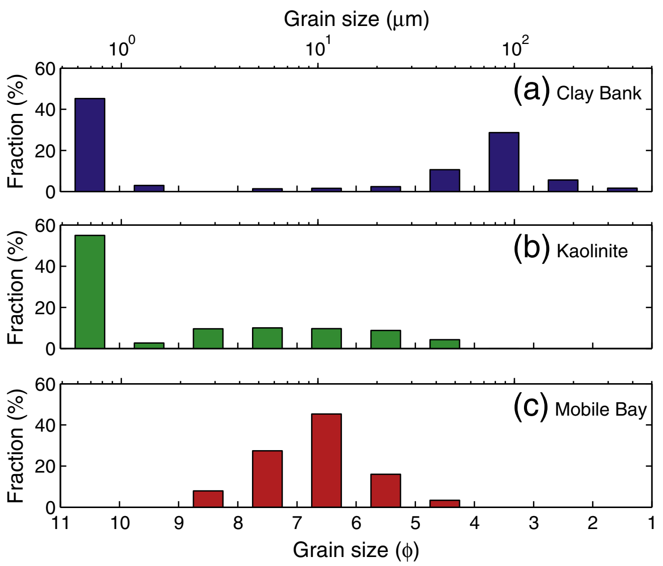

Fig. 2. Grain size distribution of the sediments used in this study (after Ha and Maa, 2010).

3.3. Laboratory measurement: SonTek's 1.5-MHz PC-ADP

Laboratory measurement consisted of two parts: the signal calibration using a mixing chamber and the SSC profiling test using a settling tank.

A Plexiglas mixing chamber (Fig. 3) housed in the Virginia Institute of Marine Science (VIMS) was used to calibrate the transducers. The lower part of the chamber is funnel-shaped to prevent sediments from accreting on the bottom. A circulation pump at the bottom end brought the water–sediment mixture through four return pipes back to the upper level of the chamber in order to accomplish a fully mixed suspension with nearly constant SSC and grain size distribution. The mixing chamber was filled with tap water and left for one day to be stabilized in the room temperature and to allow air bubbles to escape from the chamber. While the circulation pump was continuously running to make homogeneous suspension, a certain amount of sediment slurry was added to the chamber to reach a pre-determined SSC. A PC-ADP was mounted at the top of the chamber to record the profiles of backscattered signals at 2 Hz, from which 2-min ensemble averages were obtained; see Table 1 for the configuration and selected setups. To correct the slant angle of the transducers, the mount frame was purposely tilted 15° (Fig. 3), which made the beam axis normal to the chamber base and facilitated the calibration of a single transducer beam at every measurement. The tilting, however, caused the beams transmitted by the other two transducers to hit the sidewall of chamber, which might contaminate the return signals of the calibrated transducer. The values of the signal array after blocking unused transducers with wood caps showed that their effects were insignificant. Water samples were withdrawn from six sampling ports with an interval of 0.1 m, and the uppermost port was located at 0.09 m below the transducer (Fig. 3). They were vacuum filtered through pre-weighed glass fiber filters, if the

Table 2
Comparison of used sediments.

	Clay Bank		Kaolinite	Mobile Bay
Composition	Clay	Very fine sand	Pure clay	Clay and silt
d_{50} (μm)	0.7[a]	88[a]	0.7	9.8
ka	0.002	0.276	0.002	0.012
Acoustic sensitivity relative to kaolinite[b]	1	$2*10^6$	1	70

[a] Two modes are chosen due to the bimodal size distribution.
[b] Estimated using Eq. (5).

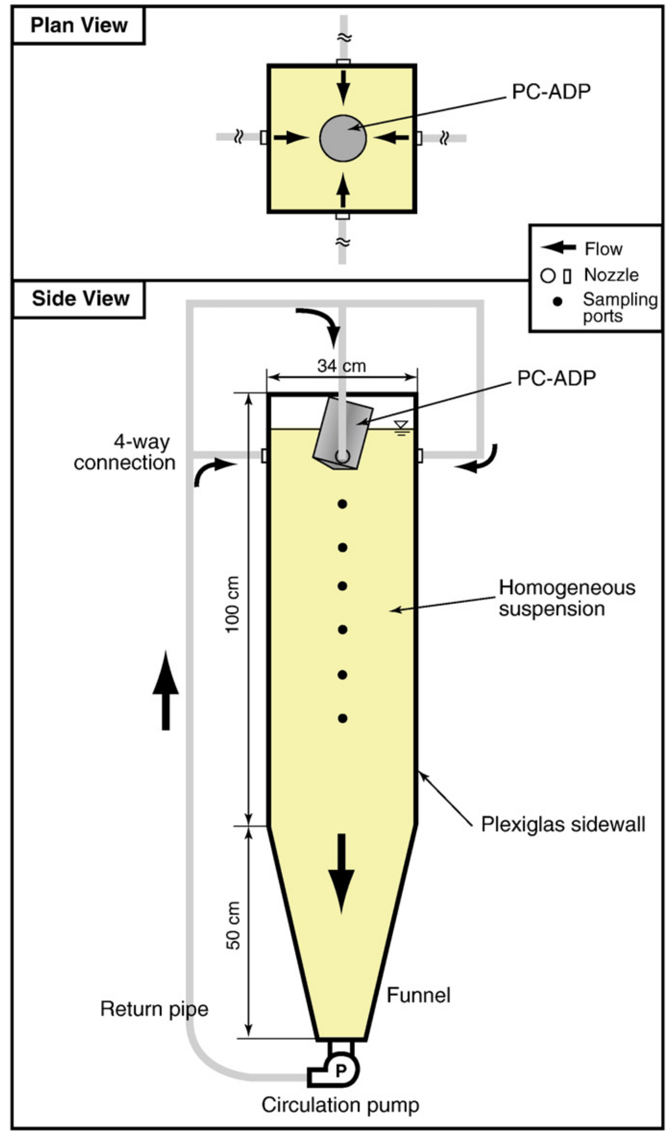

Fig. 3. Mixing chamber used for calibration of a PC-ADP. The first sampling port is located at 0.09 m from the transducer and the interval between ports is 0.1 m. Note that the PC-ADP was purposely tilted 15° to align the beam axis along the chamber.

SSC of a sample is expected to be lower than 1 g l^{-1}. If the SSC is expected to be higher than 1 g l^{-1}, pre-weighed aluminum pans were used to avoid a clogging problem in filtration. The residues on filters, or the samples in aluminum pans, were oven dried at 103–105 °C for 24 h, and then reweighed to determine the SSC. The experiment was repeated for different SSC levels in the range of 0.16–18.89 g l^{-1} for the Clay Bank sediment and 0.07–34.63 g l^{-1} for kaolinite. It is critical to maintain a homogeneous mixture in the mixing chamber. Fig. 4 shows relative SSC, a ratio of the measured SSC to the range-averaged SSC. It was concluded that the suspension in the chamber was nearly homogeneous based on the fact that most samples were within ±5–15% of mean SSC.

Once the signal calibration was completed, the SSC profiling test was conducted in a settling tank (diameter: 0.75 m, height: 1.5 m). After stirring up the water–sediment mixture by three submersible pumps, they stopped to allow suspended sediments to settle in a quiescent condition. The downward-looking PC-ADP, placed at 1.25 m above the bottom (mab), recorded the profiles of backscattered strengths at 2 Hz, with the cell size of 0.047 m and the blanking distance of 0.15 m (Table 1). For another reference, an OBS was installed at 0.9 mab, which corresponded to the fifth cell of the deployed PC-ADP. During the experiment, water samples were

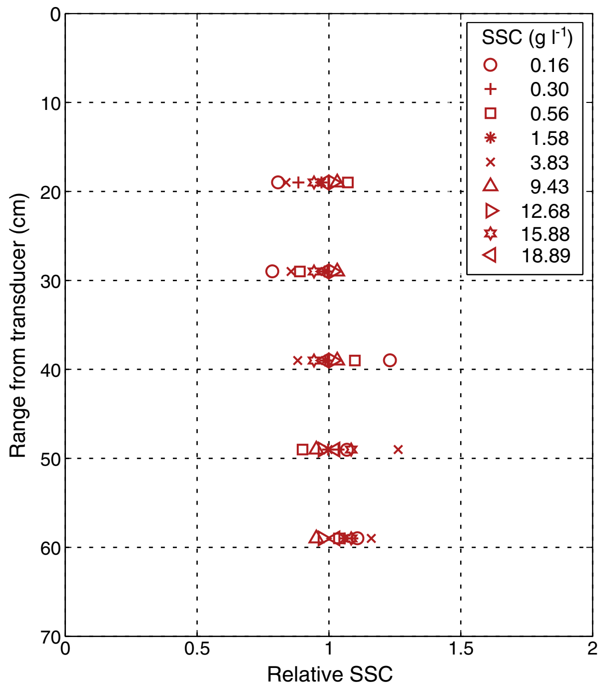

Fig. 4. Relative SSC, a ratio of the measured SSC to the range-averaged SSC, at different ranges from transducer to check homogeneity in the mixing chamber.

withdrawn at 0.1, 0.2, 0.3, 0.6 and 0.9 mab. The backscattered strengths from PC-ADP and OBS were converted to the SSCs by calibrating against the water samples. PC-ADP-derived SSC (SSC_{PCA}) was compared with OBS-derived SSC (SSC_{OBS}) and sample-derived SSC (SSC_{SAM}).

3.4. In-situ measurement: RDI's 600-kHz ADCP

A downward-looking ADCP (RDI WorkHorse Sentinel, 600 kHz) was installed on a pile in shallow Mobile Bay, Alabama (mean water depth of 3.5 m). To avoid being hit by the footprints of the four main beams, a 2-m horizontal extension arm was mounted on a pile. The ADCP was attached at the tip of the arm, and the transducers were placed at 2 mab. For high spatial resolution and accuracy, the feature of mode 11 was selected in configuration setup (Table 1). The cell size was set to 0.1 m, and the blanking distance to 0.5 m. The ADCP recorded the profiles of backscattered signals at 2 Hz, generating 5-min ensemble averages at a time increment of 1 h. Three YSI Sondes (YSI Inc., 6600EDS) were also installed at 0.15, 0.5 and 1.0 mab to record temperature, salinity, water depth and turbidity. Unfortunately, the YSI at 0.5 mab malfunctioned because of the flooded sensors. During the maintenance service for ADCP and YSIs, CTD castings were done to acquire the vertical profiles of salinity, temperature and transmission, and water samples were collected at the depths of YSI's optical sensors. The filtering procedure described in the previous section was followed to determine the SSC. The backscattered strengths from ADCP and YSI's optical turbidity sensors were converted to the SSCs through the calibration against the water samples. Like the laboratory measurement, SSC_{PCA} was compared with SSC_{OBS} and SSC_{SAM}.

3.5. Verification of acoustic signals

The OBS output from the laboratory and field measurements showed a good linear regression with water samples (Fig. 5). In assessing the errors, therefore, SSC_{PCA} was compared with SSC_{OBS}. The mean error (ME), mean absolute error (MAE) and mean relative error (MRE) were calculated by

$$ME = \frac{1}{N}\sum(SSC_{PCA} - SSC_{OBS}) \tag{4a}$$

$$MAE = \frac{1}{N}\sum\left|SSC_{PCA} - SSC_{OBS}\right| \tag{4b}$$

$$MRE(\%) = \frac{\sum|SSC_{PCA} - SSC_{OBS}|}{\sum SSC_{OBS}} \times 100 \tag{4c}$$

where N is the number of data. ME represents a bias of SSC_{PCA} with respect to SSC_{OBS}. A positive ME means the PC-ADCP's overestimation, whereas a negative ME means its underestimation. The magnitude of MAE indicates the average deviation between SSC_{PCA} and SSC_{OBS}, and MRE is the percent of MAE to the mean SSC_{OBS}. The percent of MAE relative to the range of SSC_{OBS} was also calculated to quantify the comparisons.

4. Results

4.1. Laboratory measurement in the mixing chamber: SonTek's 1.5-MHz PC-ADP

The results of the signal calibration using the mixing chamber are shown in Fig. 6 for the Clay Bank sediment and kaolinite under various SSCs. The first sampling port was inside the blanking zone of PC-ADP, and thus the data from the second ($R = 0.19$ m) to the sixth ($R = 0.59$ m) sampling ports are displayed. Note that y-axis values of $\overline{S_v}$ (see Eq. (3)) are the net volume scattering strength corrected by subtracting spreading loss and attenuation including the near-field transducer correction (Downing et al., 1995), and that at each SSC level the highest backscattered strength corresponds to the measurement at $R = 0.19$ m

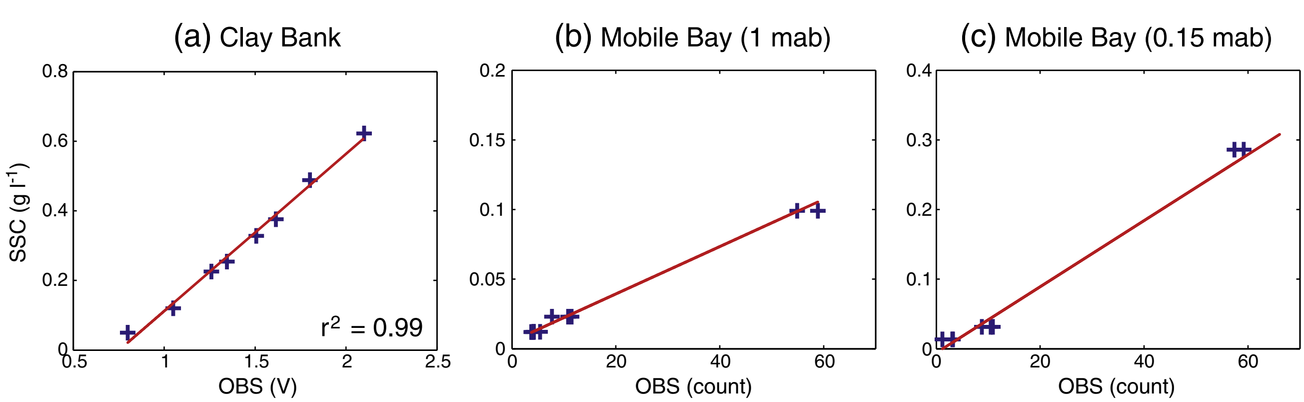

Fig. 5. Calibration of OBS: (a) Clay Bank sediment; and (b, c) Mobile Bay sediment. Due to the limited, clustered data from Mobile Bay, r^2 was not given.

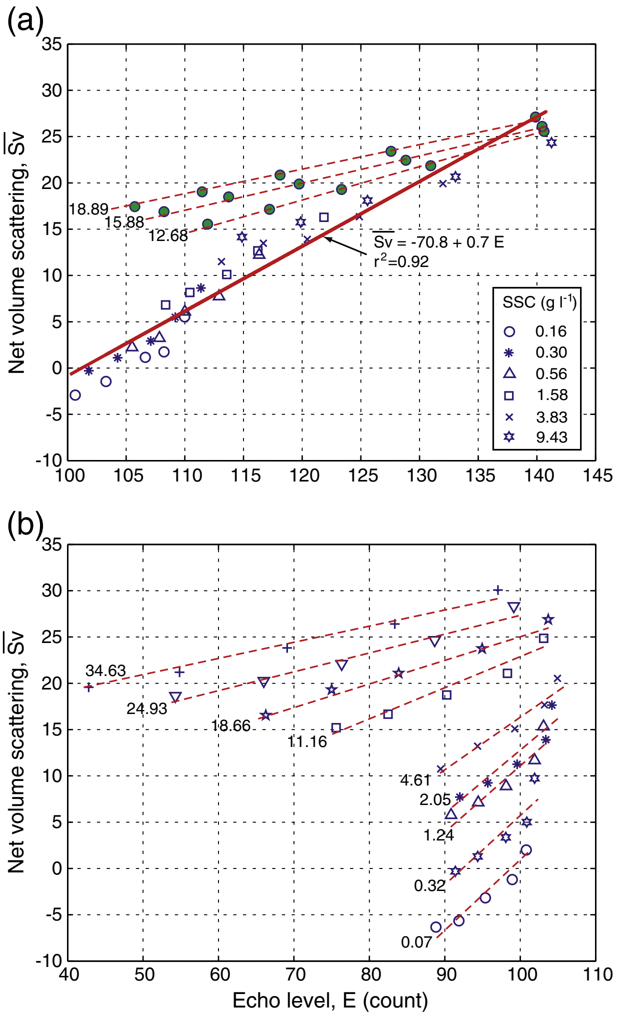

Fig. 6. Signal calibration results: (a) Clay Bank sediment; and (b) kaolinite. $\overline{S_v}$ is the net volume scattering strength corrected by subtracting spreading loss and attenuation by water and suspended particles. The numbers indicate the SSC in g l^{-1}. The solid line in (a) indicates a unified regression line for the SSC levels of 0.16–9.43 g l^{-1}. The dashed lines in (a) and (b) indicate the regression for each SSC. The lowest and highest echo levels at each SSC level indicate the signals at $R = 0.59$ and 0.19 m, respectively. Note different x-axis scales in (a) and (b).

and the lowest one the measurement at $R = 0.59$ m. The acoustic responses to the Clay Bank sediment can be divided into two groups based on the response of backscattered strength to SSC. For the first group with SSC levels of 0.16–9.43 g l^{-1}, the backscattered strength increased with increasing SSC. An individual SSC showed a good linear regression between $\overline{S_v}$and backscattered strength, with the slope (K_c) and y-intercept (C') varying little for different SSC levels. The entire data in this group can be represented by a unified linear regression with K_c of 0.7 and C' of -70.8 (solid line with $r^2 = 0.92$ in Fig. 6a). At the SSC level of 9.43 g l^{-1}, the echo level reached the overall maximum of 142 counts. The second group has SSC levels of 12.68–18.89 g l^{-1}. Each SSC level has its own linear response, but with a much smaller range of $\overline{S_v}$ (Fig. 6a). In this high SSC group, the backscattered strength at a fixed range decreased with increasing SSC due to more sound attenuation by suspended particles. For instance, the backscattered strength at $R = 0.19$ m was 112 counts for SSC = 12.68 g l^{-1}, and it decreased to 106 counts when SSC increased to 18.89 g l^{-1}. As SSC increased from 12.68 to 18.89 g l^{-1}, moreover, the $\overline{S_v}$ and C' increased but K_c (slopes of dashed lines in Fig. 6a) slightly decreased. Such responses indicate that the volume scattering ($10 \cdot \log(SSC)$), spreading loss ($10 \cdot \log(R^2)$) and sound attenuation ($2(\alpha_w + \alpha_s)R$) changed in unequal proportions with increasing SSC. That is, the volume scattering was larger than the sum of spreading loss and sound attenuation term, but the rate of increase in volume scattering was smaller than that of total sound loss (see Eq. (3)). Therefore, each regression for SSC > 9.43 g l^{-1} significantly diverged from the unified regression for the low SSC.

The kaolinite showed a similar but somewhat different acoustic response (Fig. 6b). The backscattered strengths from kaolinite were much smaller than those from the Clay Bank sediment at similar SSC levels. Although the kaolinite has the same grain size as the large portion of the Clay Bank sediment, the backscatters of sandy particles can overwhelm those of clay particles, which resulted in different acoustic responses (Fig. 6). The linear relationship between $\overline{S_v}$ and backscattered strength was observed, but different SSC levels had different regression lines. Such responses suggest that the suspended kaolinite particles may not be fully ensonified to produce the backscatters, most likely because the particle size is much smaller than the transmitted acoustic wavelength (≈1 mm). The 1.5-MHz acoustic wave is significantly attenuated in the vicinity of 2 μm in grain size (Fig. 1b), which is close to the major component of kaolinite (Fig. 2b). Due to the combined effects of weak backscattering and strong sound attenuation, less backscatter was recorded. The maximum signal saturation level was observed around 105 counts, much lower than that for the Clay Bank sediment (142 counts). This indicates that the same PC-ADP can produce different signal saturation levels depending on the sediment properties. Due to earlier signal saturation for kaolinite, the effect of increases in SSC could not fully contribute to the increases in the backscattered strength. A unified regression equation, therefore, could not be defined for kaolinite, indicating that a 1.5-MHz PC-ADP may not be an effective instrument for estimating the SSC profile of kaolinite nor such fine-grained materials. This result granted us to conduct the second test for SSC profiling only with the Clay Bank sediment.

4.2. Laboratory measurement in the settling tank: SonTek's 1.5-MHz PC-ADP

Fig. 7a shows the time series of the SSC_{PCA} profiles for the Clay Bank sediment calculated by the inversion algorithm described above. As time elapsed, the suspended sediments settled downward, and thus the SSC gradually decreased at a given elevation. Due to the blanking zone, the first cell started at a range of 0.15 m from the transducer (i.e., 1.1 mab). Inversion of the acoustic signals was verified by comparing the SSC_{PCA} profiles with the SSC_{SAM} (Fig. 7b). As a whole, good agreement existed between SSC_{PCA} and SSC_{SAM}, but the agreement at a mid level (0.6 mab) appeared slightly poorer than other levels. A better agreement existed at the beginning of the experiment when coarse and fine particles were relatively well mixed, but as time elapsed, the calibration deteriorated a little, indicating that the larger particles fell out of suspension faster than the smaller ones. This is because the transmitted acoustic wave is more sensitive to coarse particles than fine particles when the multi-class sediments are well mixed. A good correlation existed between SSC_{PCA} and SSC_{OBS} with $r = 0.96$ (Fig. 8). But a non-linear (exponential) relationship might be equally postulated. This is because the acoustic and optical instruments have different sensitivity to different grain size and the backscattered signals from two instruments independently depend on the settling rate of each size fraction. The overestimation of SSC_{PCA} might be attributed to a wide grain size spectrum with lots of fine silt and clay as well as about 50% fine sand. Because the OBS signal is proportional to the cross-sectional area of the suspended sediments, it is effectively measuring the concentration of silt and clay while the PC-ADP is seeing almost exclusively the sandy portion due to its higher acoustic sensitivity. In the early stage of the experiment when the SSC was relatively high, the particle size at 0.9 mab was larger, which resulted in an excessive increase in the acoustic backscattered strength, compared to those at later times. *MAE* and *MRE* of acoustic estimates were 0.0055 g l^{-1} and 10.5%, respectively.

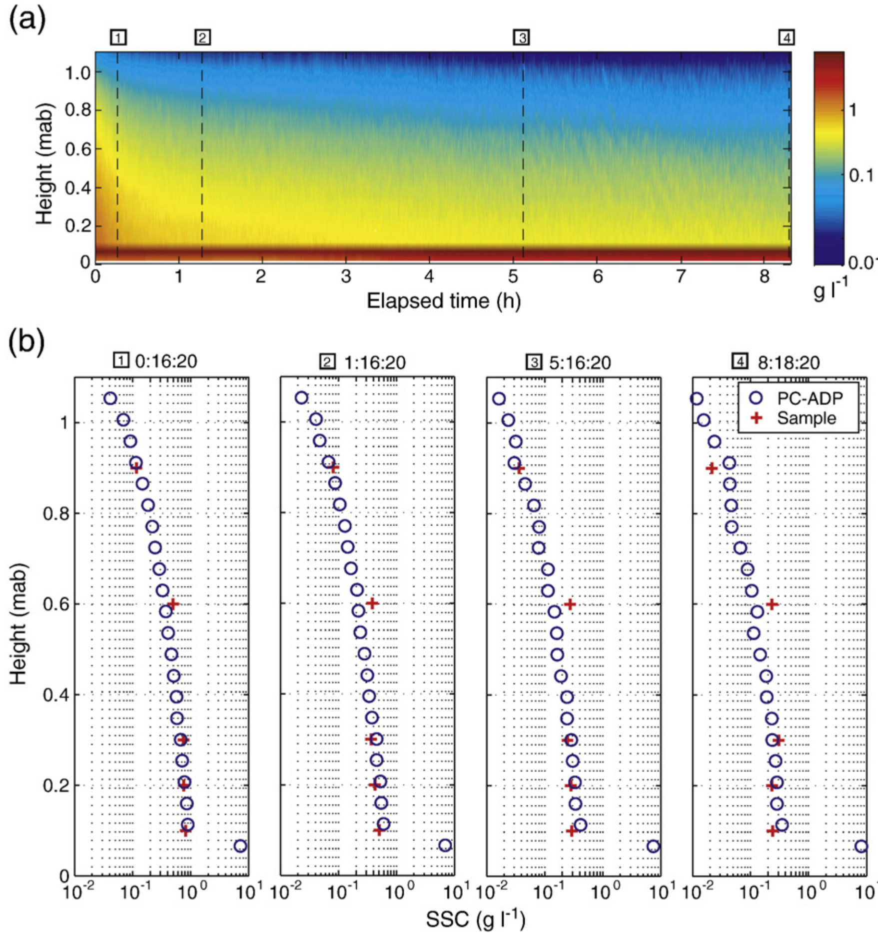

Fig. 7. (a) Time series of SSC_{PCA} profile; and (b) comparison between SSC_{PCA} and SSC_{SAM} at four instances. The numbers at the top of (b) indicates the elapsed time (hh:mm:ss) corresponding to the dashed lines in (a).

4.3. Mobile Bay measurement: RDI's 600-kHz ADCP

Fig. 9 shows the time series of the SSC_{PCA} profiles in Mobile Bay and the comparison with the time series of SSC_{OBS} at 0.15 and 1 mab. The

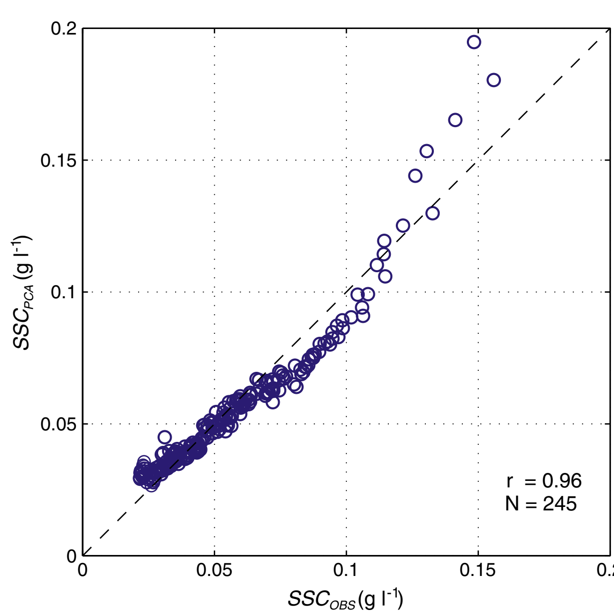

Fig. 8. Comparison between SSC_{PCA} and SSC_{OBS} at 0.9 mab (fifth cell) for the laboratory experiment. The dashed line is the unity line.

acoustic signal identified the presence of a high-concentration fluffy layer immediately over the consolidated sediment bed (the strong, near-bed echoes in Fig. 9a). Both acoustic and optical data showed the active sediment suspension caused by wind forcing. During the winter storm with strong wind stress in 338–340 days, for instance, resuspension increased the SSC at 0.15 mab to about 0.25 g l^{-1}, and the resuspended sediments extended into the water column above 1.5 mab. After the storm passed, the SSC quickly dropped to the background level (0.01–0.03 g l^{-1}), and the high SSC was observed only near the sediment bed, resulting in a typical, upward-decreasing SSC profile. This indicates that the source of suspended sediment was mainly from the erosion and resuspension of bed materials, not the lateral advective transport.

Table 3 summarizes the error statistics at 0.15 and 1 mab to evaluate the error of SSC_{PCA} with respect to SSC_{OBS}. It is noted that *MAE* and *MRE* at 0.15 mab were always larger than those at 1 mab. This is because the lower sensor elevation (e.g., 0.15 mab) would be more frequently exposed to the near-bed sediment behaviors such as erosion and deposition, resulting in higher temporal variations in particle size and SSC. The wider size spectra of suspended sediments ejected from the bottom by the strong mixing differently influenced the sensitivities of acoustic and optical backscattering, resulting in increasing the gap between the two estimates. In addition, the bias from side lobe interference near the bottom seems to be a potential reason for these larger errors at 0.15 mab (for details, see Section 5.2).

To further investigate different responses in two measuring elevations, the scatter plots for acoustic and optical estimates are shown in Fig. 10. At 1 mab, the SSC_{PCA} was underestimated ($ME = -0.0111$ g l^{-1}) compared with SSC_{OBS}, whereas the SSC_{PCA} was

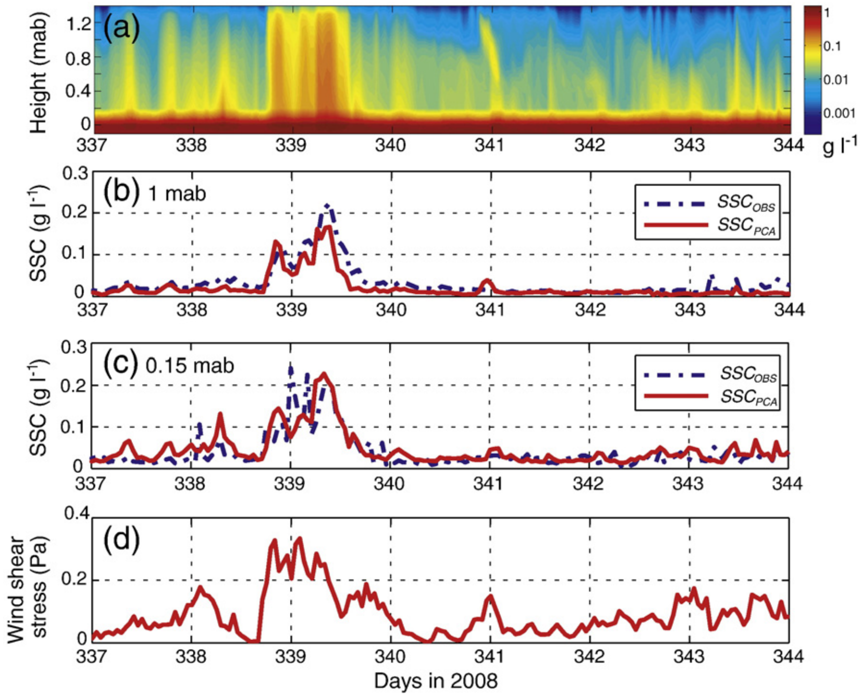

Fig. 9. Time-series data from the lower Mobile Bay: (a) SSC_{PCA} profile; (b) comparison between SSC_{PCA} and SSC_{OBS} at 1 mab; (c) comparison between SSC_{PCA} and SSC_{OBS} at 0.15 mab; and (d) wind shear stress calculated by Wu (1980).

relatively overestimated ($ME = 0.0073$ g l^{-1}) at 0.15 mab. The under/overestimation may be attributable to different sediment size spectra and their effects on the sensitivities of acoustic and optical backscattering. It is noted that the wavelength (ca. 800 nm) of OBS is much shorter than that of PC-ADCP. Although the PC-ADCP with a single frequency is not capable of addressing the changes in grain size, we can infer the relative enrichment or depletion of coarse and fine particles in suspension. The overestimation of PC-ADCP represents the fact that coarser particles (or flocs) were relatively enriched at 0.15 mab. In contrast, its underestimation represents their depletion at 1 mab. The effect of near-bed sediment population on the acoustic response is discussed below.

5. Discussion

5.1. Acoustic sensitivity to particle (or floc) size

Acoustic sensitivity (AS) to a sediment particle at a given SSC can be written as

$$AS \propto \sum_n \frac{F_n^2}{a_n} \tag{5}$$

where F is a form factor describing the scattering properties of an ensonified particle, a is the particle radius, and subscript n denotes the n-th class size (Lynch et al., 1994; Thorne and Hanes, 2002; Thorne et al., 1993; Vincent, 2007). The form factor is proportional to the square of ka where k ($=2\pi f/c$, where f is the acoustic wave frequency and c is the sound speed in water) is the wave number. The peak of acoustic sensitivity occurs when the circumference of particle, assuming a spherical shape, is close to the acoustic wavelength, i.e., $ka \approx 1$ (Thorne and Hanes, 2002). Because c is about 1500 m s^{-1} in water, the values of ka for the Clay Bank sediment are approximately 0.002 and 0.276 for clay and very fine sand portions, respectively, whereas those for kaolinite and Mobile Bay sediment are about 0.002 and 0.012, respectively (Table 2). For the Clay Bank sediment, two very different ka values indicate that the majority of backscatters were produced by the very fine sand portion, and that the contribution of the clay portion was negligible. Therefore, the acoustic sensitivity of very fine sand of the Clay Bank sediment is about six orders of magnitude larger than that of kaolinite (Table 2). That is, kaolinite clay is too small to be effectively detected by the wavelength of transmitted 1.5-MHz acoustic signals (≈ 1 mm), and thus the performance of PC-ADP with kaolinite is not warranted (Fig. 6b). The Clay Bank sediment showed lower MAE (0.0055 g l^{-1}), MRE (10.5%) and MAE to C_{OBS} range (4.1%), when compared with those of Mobile Bay sediment. This is because the acoustic sensitivity of the Clay Bank sediment, particularly that of the very fine sand, is several orders of magnitude larger than that of Mobile Bay sediment (Table 2).

If the operating frequency is doubled, the detectable particle radius can be theoretically reduced by half. The tradeoff between frequency and SSC-dependent sound attenuation, however, should be considered to acquire an optimal output. SonTek (1997) provided a rough guideline that the marginal value of ka may be about 0.05 to detect suspended sediment particles. The Mobile Bay measurement, however, demonstrated that the PC-ADCP may work well even for $ka = 0.012$.

All the sediments used in this study include a fine particle portion, which is characterized by cohesiveness. In most cases, the sediments with this fine-grained portion tend to aggregate into flocs (Manning and Dyer, 1999; Sanford et al., 2005; Shao et al., in press; van Leussen,

Table 3
Error statistics of SSC_{PCA} with respect to SSC_{OBS}.

	Clay Bank	Mobile Bay	
	0.9 mab	0.15 mab	1 mab
ME (g l^{-1})	−0.0002	0.0073	−0.0111
MAE (g l^{-1})	0.0055	0.0174	0.0133
MRE (%)	10.5	45.8	41.6
MAE to SSC_{OBS} range (%)	4.1	7.3	6.2
Mean SSC_{OBS} (g l^{-1})	0.0524	0.0380	0.0321
SSC_{OBS} range (g l^{-1})	0.1346	0.2400	0.2157

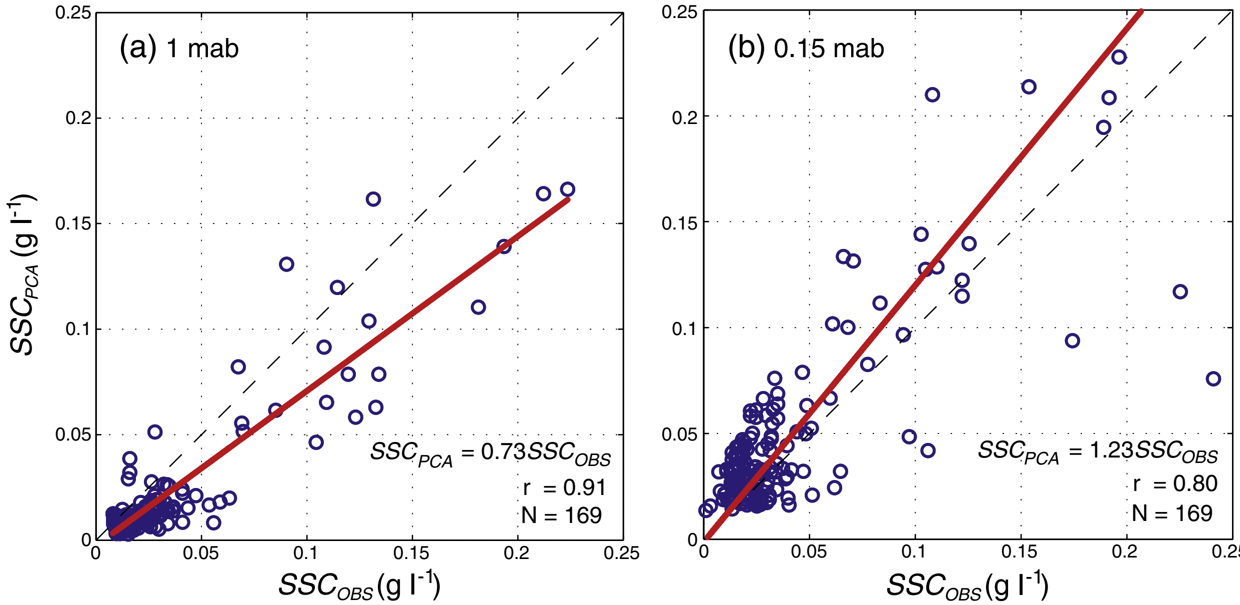

Fig. 10. Comparison between SSC_{PCA} and SSC_{OBS} at (a) 1 mab and (b) 0.15 mab in the lower Mobile Bay.

1988). When flocs are present in the water column, it is not clearly understood whether acoustic backscatter responds to flocs as a whole bound or individual primary particles therein. Based on the theoretical relationship between the acoustic wavelength and the particle size, it has been suggested that the acoustic signal may penetrate the pores of flocs, and thus the response is more dependent on the properties (e.g., size and concentration) of primary particles rather than those of flocs (Fugate and Friedrichs, 2002). Although the present study does not provide direct evidence, the findings from the Mobile Bay field experiment depict a somewhat different pattern from what was previously proposed. Compared with OBS, for instance, the PC-ADCP overestimated SSC in the near-bed level (0.15 mab), while it underestimated SSC in the higher level (1 mab) (Fig. 10). Given that these outcomes are from the same instrument, the higher response of acoustic backscatter indicates higher acoustic sensitivity, and thus larger form factor. When considered that the sensitivity reaches the peak at $ka \approx 1$, the strongest acoustic response can be observed with the sediment size of about 400 μm. This suggests that the suspended sediments at 0.15 mab might have more fractions of particles close to this maximum responsive size compared to those at 1 mab.

Furthermore, the higher responsiveness in the near-bed layer may result from the introduction of larger flocs eroded and resuspended from the bed, which likely implies that the PC-ADCP responds to these flocs as a whole bound. Using in-situ video data collected from Chesapeake Bay, Kim and Sanford (2009) showed that larger flocs (several hundred μm) can be produced in BBL during the erosion phase. Flocs eroded from the bed, i.e., bed aggregates, are more compacted and robust than normal flocs aggregated in the water column, which may allow bed aggregates to survive during the resuspension processes. This is also consistent with the findings of Smith and Friedrichs (2010) that bed aggregates ($\rho_f = 1200–1800$ kg m^{-3} where ρ_f is floc density) have higher density than normal flocs ($\rho_f = 1025–1200$ kg m^{-3}). A presently open question is "what is a critical density of a floc so that it can be acoustically detected as a single grain?" Based on the near-bed acoustic responses shown in Fig. 10b, it can be inferred that such an acoustic detection threshold may be somewhere in the density range of bed aggregates, and that flocs are more likely to be acoustically detected as a whole bound as ρ_f increases. The concurrent measurement of floc size and density using a LISST-100 laser particle sizer and a floc camera (e.g., Mikkelsen et al., 2005; Smith and Friedrichs, 2010) can provide direct evidence to resolve this issue, which is worthy for future studies.

5.2. Uncertainties and error sources

The inverting processes from the acoustic signal to SSC using a simplified sonar equation have inherent uncertainties and errors in measurement and data analysis. First, in the signal inversion algorithm, it is assumed that the spatial and temporal distributions of sediment grain size might remain constant. For practical applications, a single value, d_{50}, of particle size has been usually used to iteratively calculate the sound attenuation coefficients and SSCs for all profiling cells. In the case of multi-modal sediment that cannot be regarded as one single population, however, d_{50} is not a good representative. Thus, a biased result is expected when d_{50} is used for the acoustic inversion processes of field data where sediment grain size distribution would continuously change in time and space. In addition, ADCP or PC-ADCP with a single frequency is not capable of resolving whether changes in backscattered strength are associated with changes in SSC or those in particle size distribution, i.e., changes in grain size can be misinterpreted as changes in SSC (Ha et al., 2009; Reichel and Nachtnebel, 1994). However, these uncertainties related to the particle size can be partly solved by employing instruments with multiple frequencies (Crawford and Hay, 1993; Hay and Sheng, 1992; Smerdon, 1996). It is promising that manufacturers are developing multi-frequency ADCP that can concurrently transmit different frequencies with harmonic interference (SonTek, pers. comm.).

Second, the ADCP or PC-ADCP has a slanted (15–30°) beam pattern, which is inevitable to resolve three components of flow velocities and to ensure that main lobes (typically, 3 or 4) do not overlap so that the sampling volumes from each transducer are separated. In the downward-looking setup, however, this feature results in an angled intersection with the sediment bed, producing the unwanted boundary echoes from side lobes while main lobes are still propagating in the water column. The same problem occurs at water surface in an upward-looking setup. Although the side lobes have much lower acoustic energy than the main lobes, the reflected signal from an interface between media with different densities is much stronger than the backscattered signal from suspended particles. Thus, the last 3–14% of the entire profile, depending on a slant angle, has a potential to be interfered by side lobe effects (Land and Jones, 2001; RDI, 1996; SonTek, 2001a; Wall et al., 2006). This side lobe interference is another likely explanation for the overestimation of SSC near the bed shown in Fig. 10. Since the percent of the main lobe that is not interfered with side lobes is proportional to the cosine of slant angle, an ABS with narrow, vertical (i.e., no slant angle) beam can solve such a side lobe interference (Aquatec, pers. comm.).

Finally, there are several factors not included in the simplified sonar equation. Measurement errors may arise from the scattering of unwanted target such as air bubbles or organisms (Kinsler et al., 2000). Since they have higher acoustic impedance than mineral sediments, a strong scatter wave generated can be easily detected by the transducer (Greinert and Nutzel, 2004). Unfortunately, it is impossible to quantitatively differentiate between suspended sediments and air bubbles or organisms in natural environments. Precaution should be, therefore, taken to avoid their effects on backscatter when such issues have been reported in a deployed site.

6. Conclusions

The capability of two commercially available PC-ADCPs was evaluated for estimating SSC profiles in BBL. The following conclusions were drawn from this study.

(1) A natural sediment sample from Clay Bank, a mixture of clay and very fine sand, showed a good linear relationship ($r^2=0.92$) between range-corrected volume scattering and backscattered strength until SSC increased up to about 10 g l^{-1}. PC-ADCP was able to measure SSC profiles up to that level without any problem related to the severe sound attenuation and signal saturation. In contrast, a commercially available kaolinite showed earlier signal saturation and non-unified linear regressions between range-corrected volume scattering and backscattered strength, most likely because the particle size is much smaller than the transmitted acoustic wavelength.

(2) For the mixture of clay and sand like the Clay Bank sediment, the PC-ADCP's backscattered strength is more affected by sandy particles rather than muddy particles because the sound is backscattered most efficiently by particles of which size is the closest to the emitted acoustic wavelength. In evaluating the acoustic sensitivity to multi-modal sediment, d_{50} is not a good representative. Instead, the particle size that exhibits the largest acoustic sensitivity should be used in the acoustic inversion algorithm to correctly account for the sound scattering and absorption by suspended sediments.

(3) The BBL measurement in Mobile Bay showed that the PC-ADCP-derived concentration was relatively overestimated at near-bed level (0.15 mab) because the acoustic sensitivity is enhanced by the coarser particles and denser bed aggregates that can be acoustically detected as a single grain rather than many small primary particles. The side lobe interference near the bottom is also a plausible reason for this overestimation.

(4) *MAE* between the acoustic and optical estimates in Mobile Bay was within 4.1–7.3% of the OBS-derived concentration range, and *MRE* was within 10.5–45.8%. Such errors are attributable to the different acoustic and optical scattering responses to given sediment size spectra. This study suggests that the PC-ADCP has potential use for revealing the evolution of in-situ near-bed suspension with high vertical and temporal resolutions.

Acknowledgements

This study was supported by the VIMS Graduate Research Grant and Fisheries Oceanography in Coastal Alabama at DISL funded by Alabama Department of Conservation and Natural Resources — Marine Resources Division. The final preparation of manuscript was supported by the KOPRI Grant (PE10260) for new scientists. Y. Ma helped to carry out the laboratory experiments. C. Friedrichs and B. Dzwonkowski meticulously reviewed the draft of this paper. We thank K. Weis, N. Nazarian, L. Linn and A. Gunter for the technical support during the field surveys. The constructive comments by two anonymous reviewers and D.J.W. Piper are sincerely appreciated.

References

Admiraal, D.M., Garcia, M.H., 2000. Laboratory measurement of suspended sediment concentration using an Acoustic Concentration Profiler (ACP). Experiments in Fluids 28, 116–127.

Aquatec, 2006. The AQUAscat 1000 acoustic backscatter system. http://www.aquatecgroup.com/download/datasheet/aquascat/AQUAscat1000.pdf.

Betteridge, K.F.E., Thorne, P.D., Cooke, R.D., 2008. Calibrating multi-frequency acoustic backscatter systems for studying near-bed suspended sediment transport processes. Continental Shelf Research 28 (2), 227–235.

Crawford, A.M., Hay, A.E., 1993. Determining suspended sand size and concentration from multifrequency acoustic backscatter. Journal of the Acoustical Society of America 94 (6), 3312–3324.

Deines, K.L., 1999. Backscatter estimation using broadband acoustic Doppler current profilers. Proceedings of the 6th IEEE Working Conference on Current Measurement. San Diego, CA, pp. 249–253.

Downing, J., 2006. Twenty-five years with OBS sensors: the good, the bad and the ugly. Continental Shelf Research 26, 2299–2318.

Downing, J.P., Beach, R.A., 1989. Laboratory apparatus for calibrating optical suspended solids sensors. Marine Geology 86, 243–249.

Downing, A., Thorne, P.D., Vincent, C.E., 1995. Backscattering from a suspension in the near field of a piston transducer. Journal of the Acoustical Society of America 97 (3), 1614–1620.

Fisher, F.H., Simmons, V.P., 1977. Sound absorption in sea water. Journal of the Acoustical Society of America 62 (3), 558–564.

Friedrichs, C.T., Wright, L.D., Hepworth, D.A., Kim, S.C., 2000. Bottom-boundary-layer processes associated with fine sediment accumulation in coastal seas and bays. Continental Shelf Research 20, 807–841.

Fugate, D.C., Friedrichs, C.T., 2002. Determining concentration and fall velocity of estuarine particle populations using ADV, OBS and LISST. Continental Shelf Research 22, 1867–1886.

Gartner, J.W., 2004. Estimating suspended solids concentrations from backscatter intensity measured by acoustic Doppler current profiler in San Francisco Bay, California. Marine Geology 211, 169–187.

Greinert, J., Nutzel, B., 2004. Hydroacoustic experiments to establish a method for the determination of methane bubble fluxes at cold seeps. Geo-Marine Letters 24, 75–85.

Ha, H.K., 2008. Acoustic measurements of cohesive sediment transport: suspension to consolidation. Ph.D. Dissertation, College of William and Mary, Williamsburg, VA, 152 p.

Ha, H.K., Maa, J.P.-Y., 2009. Evaluation of two conflicting paradigms for cohesive sediment deposition. Marine Geology 265, 120–129.

Ha, H.K., Maa, J.P.-Y., 2010. Effects of suspended sediment concentration and turbulence on settling velocity of cohesive sediment. Geosciences Journal 14 (2), 163–171.

Ha, H.K., Hsu, W.-Y., Maa, J.P.-Y., Shao, Y., Holland, C.W., 2009. Using ADV backscatter strength for measuring suspended cohesive sediment concentrations. Continental Shelf Research 29, 1310–1316.

Hamilton, L.J., Shi, Z., Zhang, S.Y., 1998. Acoustic backscatter measurements of estuarine suspended cohesive sediment concentration profiles. Journal of Coastal Research 14 (4), 1213–1224.

Hanes, D.H., Vincent, C.E., Huntley, D.A., Clarke, T.L., 1988. Acoustic measurements of suspended sand concentration in the C2S2 experiment at Stanhope Lane, Prince Edward Island. Marine Geology 81, 185–196.

Hay, A.E., Sheng, J., 1992. Vertical profiles of suspended sand concentration and size from multifrequency acoustic backscatter. Journal of Geophysical Research 97 (C10), 15661–15677.

Hill, D.C., Jones, S.E., Prandle, D., 2003. Derivation of sediment resuspension rates from acoustic backscatter time-series in tidal waters. Continental Shelf Research 23, 19–40.

Holdaway, G.P., Thorne, P.D., Flatt, D., Jones, S.E., Prandle, D., 1999. Comparison between ADCP and transmissometer measurements of suspended sediment concentration. Continental Shelf Research 19, 421–441.

Kawanisi, K., Yokosi, S., 1997. Characteristics of suspended sediment and turbulence in a tidal boundary layer. Continental Shelf Research 17 (8), 859–875.

Kim, Y.H., Sanford, L.P., 2009. Variability of Floc Properties in Chesapeake Bay: Observation and Modeling. Proceedings of International Conference of Cohesive Sediment Transport. Rio de Janeiro/Paraty, Brazil, pp. 76–78.

Kim, Y.H., Voulgaris, G., 2003. Estimation of Suspended Sediment Concentration in Estuarine Environments Using Acoustic Backscatter from an ADCP. Proceedings of Coastal Sediments '03. CD-ROM. World Scientific Corporation and East Meat West Production, Clearwater Beach, FL.

Kim, Y.H., Gutierrez, B., Nelson, T., Dumars, A., Maza, M., Perales, H., Voulgaris, G., 2004. Using the acoustic Doppler current profiler (ADCP) to estimate suspended sediment concentration. Technical Report CPSD #04-01, Department of Geological Sciences, University of South Carolina, SC, 20 p.

Kineke, G.C., Sternberg, R.W., 1992. Measurements of high concentration suspended sediments using the optical backscatterance sensor. Marine Geology 108, 253–258.

Kinsler, L.E., Frey, A.R., Coppens, A.B., Sanders, J.V., 2000. Fundamentals of Acoustics. John Wiley and Sons Ltd., NJ. 548 p.

Lacy, J.R., Sherwood, C.R., 2004. Accuracy of a pulse-coherent acoustic Doppler profiler in a wave-dominated flow. Journal of Atmospheric and Oceanic Technology 21, 1448–1461.

Land, J.M., Jones, P.D., 2001. Acoustic measurement of sediment flux in rivers and near-shore waters. In: The 7th Federal Interagency Sedimentation Conference, Reno, NV, pp. III 127–134.

Land, J.M., Kirby, R., Massey, J.B., 1997. Developments in the combined use of acoustic Doppler current profiler and profiling siltmeters for suspended solids monitoring. In: Burt, N., Parker, R., Watts, J. (Eds.), Cohesive Sediments. John Wiley and Sons Ltd., NJ, pp. 187–196.

Lee, T.H., Hanes, D.H., 1995. Direct inversion method to measure the concentration profile of suspended particles using backscattered sound. Journal of Geophysical Research 100 (C2), 2649–2657.

Lhermitte, R., Serafin, R., 1984. Pulse-to-pulse coherent Doppler sonar signal processing techniques. Journal of Atmospheric and Oceanic Technology 1, 293–308.

Lohrmann, A., Hackett, B., Roed, L.P., 1990. High resolution measurements of turbulence, velocity and stress using a pulse-to-pulse coherent sonar. Journal of Atmospheric and Oceanic Technology 7, 19–37.

Lorke, A., Wuest, A., 2005. Application of coherent ADCP for turbulence measurements in the bottom boundary layer. Journal of Atmospheric and Oceanic Technology 22, 1821–1828.

Lynch, J.F., Irish, J.D., Sherwood, C.R., Agrawal, Y.C., 1994. Determining suspended sediment particle size information from acoustical and optical backscatter measurements. Continental Shelf Research 14, 1139–1165.

Manning, A.J., Dyer, K.R., 1999. A laboratory examination of floc characteristics with regard to turbulent shearing. Marine Geology 160 (1–2), 147–170.

Medwin, H., Clay, C.S., 1998. Fundamentals of Acoustical Oceanography. Academic Press, NY. 721 p.

Mikkelsen, O.A., Hill, P.S., Milligan, T.G., Chant, R.J., 2005. In situ particle size distributions and volume concentrations from a LISST-100 laser particle sizer and a digital floc camera. Continental Shelf Research 25, 1959–1978.

Mouraenko, O.A., 2004. Acoustic measurement techniques for suspended sediment and bedforms. Ph.D. Dissertation, University of Florida, Gainesville, FL, 150 p. near Baimao Shoal in Changjiang Estuary. Journal of Hydraulic Engineering.

RDI, 1996. Acoustic Doppler Current Profiler: Principle of Operation a Practical Primer. RD Instruments, San Diego, CA. 52 p.

RDI, 2002. High Resolution Water Profiling Water Mode 11. Application Note (FAS-013). RD Instruments, San Diego, CA. 6 p.

RDI, 2003. Use of Teledyne RD Instruments “Pulse to Pulse Coherent Mode” to Study Shear in the Wave Orbital Bottom Boundary. Technical Tips. RD Instruments, San Diego, CA. 3 p.

Reichel, G., Nachtnebel, H.P., 1994. Suspended sediment monitoring in a fluvial environment: advantages and limitations applying an acoustic Doppler current profiler. Water Research 28 (4), 751–761.

Richards, S.D., Heathershaw, A.D., Thorne, P.D., 1996. The effect of suspended particulate matter on sound attenuation in seawater. Journal of Acoustical Society of America 100 (3), 1447–1450.

Sanford, L.P., Dickhudt, P.J., Rubiano-Gomez, L., Yates, M., Suttles, S.E., Friedrichs, C.T., Fugate, D.D., Romine, H., 2005. Variability of suspended particle concentrations, sizes, and settling velocities in the Chesapeake Bay turbidity maximum. In: Droppo, I.G., Leppard, G.G., Liss, S.N., Milligan, T.G. (Eds.), Flocculation in Natural and Engineered Environment Systems. CRC Press, Washington D.C., pp. 211–356.

Shao, Y.Y., Yan, Y.X., Maa, J.P.-Y., (in press) In-situ measurements of settling velocity near Baimao Shoal in Changjiang Estuary. Journal of Hydraulic Engineering, ASCE.

Shi, Z., Ren, L.F., Hamilton, L.J., 1999. Acoustic profiling of fine suspension concentration in the Changjiang Estuary. Estuaries 22 (3A), 648–656.

Smerdon, A.M., 1996. AQ59: C-ABS System User Manual. Aquatec Electronics Ltd., Hartley Wintney, Hampshire, UK.

Smith, S.J., Friedrichs, C.T., 2010. Size and settling velocities of cohesive flocs and suspended sediment aggregates in a trailing suction hopper dredge plume. Continental Shelf Research. doi:10.1016/j.csr.2010.04.002.

Smyth, C., Hay, A.E., Zedel, L., 2002. Coherent Doppler profiler measurements of near-bed suspended sediment fluxes and the influence of bed forms. Journal of Geophysical Research 107 (C8), 19-1–19-20.

SonTek, 1997. SonTek Doppler current meters-using signal strength data to monitor suspended sediment concentration. SonTek/YSI Inc., San Diego, CA. 7 p.

SonTek, 2001a. Acoustic Doppler Profiler Technical Documentation. SonTek/YSI Inc., San Diego, CA. 186 p.

SonTek, 2001b. PC-ADP principles of operation. Technical Note, SonTek/YSI Inc., San Diego, CA, 12 p.

Sternberg, R.W., Johnson, R.V., Cacchione, D.A., Drake, D.E., 1986. An instrument system for monitoring and sampling suspended sediment in the benthic boundary layer. Marine Geology 71, 187–199.

Sutherland, T.F., Lane, P.M., Amos, C.L., Downing, J., 2000. The calibration of optical backscatter sensors for suspended sediment of varying darkness levels. Marine Geology 162, 587–597.

Thorne, P.D., Hanes, D.M., 2002. A review of acoustic measurement of small-scale sediment processes. Continental Shelf Research 22 (4), 603–632.

Thorne, P.D., Vincent, C.E., Hardcastle, P.J., Rehman, S., Pearson, N., 1991. Measuring suspended sediment concentrations using acoustic backscatter devices. Marine Geology 98 (1), 7–16.

Thorne, P.D., Manley, C., Brimelow, J., 1993. Measurements of the form function and total scattering cross section for a suspension of spheres. Journal of Acoustical Society of America 93 (1), 243–248.

Traykovski, P., Wiberg, P.L., Geyer, W.R., 2007. Observations and modeling of wave-supported sediment gravity flows on the Po prodelta and comparison to prior observations from the Eel shelf. Continental Shelf Research 27 (3–4), 375–399.

Urick, R.J., 1983. Principles of Underwater Sound. McGraw-Hill, NY. 423 p.

van Leussen, W., 1988. Aggregation of particles, settling velocity of mud flocs: a review. In: Dronker, J., van Leussen, W. (Eds.), Physical Processes in Estuaries. Spriner-Verlag, Berlin, pp. 347–403.

Vincent, C.E., 2007. Measuring suspended sand concentration using acoustic backscatter: a critical look at the errors and uncertainties. In: Balson, P.S., Collins, M.B. (Eds.), Coastal and Shelf Sediment Transport: Geological Society of London, Special Publication, 274, pp. 7–16.

Wall, G.R., Nystrom, E.A., Litten, S., 2006. Use of an ADCP to compute suspended-sediment discharge in the tidal Hudson River, New York. U.S. Geological Survey Scientific Investigations Report 2006-5055. 16 p.

Wren, D.G., Barkdoll, B.D., Kuhnle, R.A., Derrow, R.W., 2000. Field techniques for suspended-sediment measurement. Journal of Hydraulic Engineering 126, 97–104.

Wu, J., 1980. Wind-stress coefficients over sea surface near neutral conditions — a revisit. Journal of Physical Oceanography 10, 727–740.

Zedel, L., Hay, A.E., Cabrera, R., Lohrmann, A., 1996. Performance of a single-beam pulse-to-pulse coherent Doppler profiler. IEEE Journal of Oceanic Engineering 21 (3), 290–297.